Physica Medica 65 (2019) 137–142

Contents lists available at ScienceDirect

Physica Medica

journal homepage: www.elsevier.com/locate/ejmp

Original paper

Using a neural network to predict deviations in mean heart dose during the treatment of left-sided deep inspiration breath hold patients

Ciaran Malone*, Lynda Fennell, Tracy Folliard, Colin Kelly

St. Luke's Radiation Oncology Network, Ireland

ARTICLE INFO

Keywords:
Mean heart dose
Radiotherapy
Breast cancer
Deep inspiration breath hold
Machine learning
Keras
Neural network

ABSTRACT

Purpose: We investigated if a neural network could be used to predict the change in mean heart dose when a patient's heart deviates from its planned position during radiotherapy treatment.

Methods: Predictions were made based on parameters available at the time of treatment planning. The dose prescription, deep inspiration breath-hold (DIBH) amplitude, heart volume, lung volume, V90% and mean heart dose were used to predict the increase in dose to the heart when a shift towards the treatment field was undertaken. The network was trained using 3 mm, 5 mm and 7 mm shifts in heart positions for 50 patients' giving 150 data points in total. The neural network architecture was also varied to find the most optimal network design. The final neural network was then tested using cross-validation to evaluate the model's ability to generalise to new data.

Results: The optimal neural network found was comprised of a single hidden layer of 30 neurons. Based on twenty train/test splits, 94% of all prediction errors were below 0.2 Gy, 97.3% were below 0.3 Gy and 100% were below 0.5 Gy. The average RMSE and maximum prediction error over all train/test splits were 0.13 Gy and 0.5 Gy respectively.

Conclusions: Our approach using a neural network provides a clinically acceptable estimate of the increase in Mean Heart Dose (MHD), without the need for further imaging, contouring or evaluation. The trained neural network gives clinicians the information and tools required to evaluate what shift in heart position would be acceptable and which scenarios require immediate action before treatment continues.

1. Introduction

As medical technology advances, the volume of patient data accrued through diagnosis and treatment is growing substantially. As a result, there is increasing use of machine learning in radiotherapy using methods currently employed by large companies such as Google and Facebook [1–3]. Machine learning algorithms have been used to correlate image-based features with disease detection, diagnosis and clinical outcomes [4–9], to automatically segment structures [10–13], to predict tumour motion [14,15], to process medical images [16] and to predict QA results [17–19]. However, clinical adoption has been slow due to the high barrier to understanding these complex models, which are commonly considered “black boxes” to most clinicians [2]. In order to build confidence in the use of machine learning, models should be clearly described and also robustly evaluated using cross-validation methods to improve prediction performance and generalization to external data [1,2,20]. The model prediction accuracy should also be related back to clinical data, allowing the easy interpretation of the likelihood and clinical impact of an incorrect prediction [2].

Breast cancer is the most common form of cancer among women world-wide [21], resulting in a large volume of data being available for machine learning. Radiotherapy has been shown to reduce the rate of breast cancer recurrence and breast cancer death if undertaken after surgery [22,23]. However, it also involves the irradiation of normal tissues which can be minimised, but not eliminated, using modern treatment and imaging techniques [24]. One of the primary organs at risk (OAR) for left-sided breast cancer patients is the heart. As breast cancer patients have a relatively good life expectancy, keeping the heart dose as low as possible becomes a key factor in minimising cardiovascular disease [25,26]. Published literature suggests that for left breast radiotherapy treatments, the heart should receive a Mean Heart Dose (MHD) of 1–5 Gy [27–31]. The UK consensus statements for post-operative radiotherapy in breast cancer state that the majority of left breast patients should be treated to a MHD < 2 Gy [32]. Darby et al related the MHD to clinical risk and found that the rate of major cardiac events increases linearly with the MHD by 7.4% per Gray [33].

* Corresponding author at: St. Luke's Radiation Oncology Network, Dublin, Ireland.
E-mail addresses: Ciaran.malone@slh.ie (C. Malone), Lynda.Fennell@slh.ie (L. Fennell), Tracy.Folliard@slh.ie (T. Folliard), Colin.Kelly@slh.ie (C. Kelly).

https://doi.org/10.1016/j.ejmp.2019.08.014
Received 22 December 2018; Received in revised form 10 August 2019; Accepted 15 August 2019
Available online 26 August 2019

For left-sided patients, mean heart dose is related to the distance between the heart and the treatment field and this distance can be maximised using prone or Deep Inspiration Breath Hold (DIBH) treatment techniques [31,34,35]. Studies have attempted, with varying results, to formalise this relationship using a metric called the maximum heart distance, defined as a measure of the portion of heart encroaching the treatment field [27,28,36]. However, these results are difficult to generalise for clinical use when a deviation in heart position is noted during treatment. We investigated if a neural network could be used to predict the change in planned MHD when the heart changes position during treatment, based on parameters available at the time of treatment planning. There are a wide variety of machine learning approaches available. However, for this study an artificial neural network was chosen due to its ability to model both linear and non-linear relationships. The steps taken to optimize the network architecture are outlined and results compared to previous literature where more traditional prediction methods were utilised.

2. Methods

2.1. Data

Retrospective data from 50 left-breast DIBH patients treated with a tangential beam arrangement in the head-first supine position were included in this study. To generate data to train, optimise and test our model, each patient's heart structure was shifted 3 mm, 5 mm and 7 mm and the mean heart dose recorded for each shift, resulting in a total of 150 data points. To generate each shifted heart structure, the heart was initially expanded uniformly by 3 mm, 5 mm and 7 mm using Varian Eclipse's contouring tools (Varian Medical Systems, Palo Alto, CA, USA). These expanded structures were then used as a guide to shift the heart in a consistent manner towards the treatment field, as shown in Fig. 1.

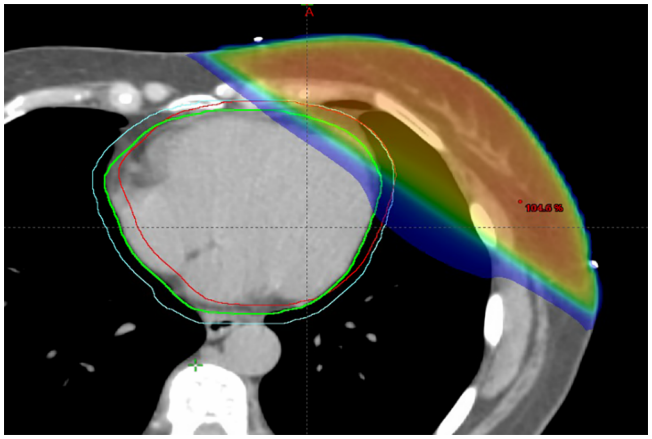

Fig. 1. Left sided DIBH breast treatment region. The original heart is shown in green, expanded heart in cyan and shifted heart in red. The delivered dose is shown as a dose wash.

Changes in heart density were considered as each shifted heart would now contain lung density pixels. Shifted heart structures were assigned a density equivalent to the average heart density measured using the CT image data. The MHD was then re-calculated and compared to the original structure's MHD before density assignment. It was found that assigning a tissue equivalent density decreased the MHD in all cases and depended on the magnitude of the shift, e.g. the greater the shift the more lung density pixels required density re-assignment and the greater the decrease in MHD. The decrease was found to be −0.11 Gy +/–0.2 Gy (1SD). As the unassigned heart slightly overestimates the MHD, it was considered appropriate to use as a conservative estimate due to the inherent uncertainty of contouring, MV imaging and intrafraction motion.

Table 1
Summary of the continuous parameters used to train the neural network.

	DIBH Amplitude (cm)	Heart Volume (cc)	Lung Volume (cc)	V90% (cc)	Planned MHD (Gy)
Count	150.0	150.0	150.0	150.0	150.0
Mean	1.0	649.8	2019.6	1400.8	1.27
Stdev	0.4	126.0	495.8	595.6	0.53
Min	0.3	469.4	863.4	467.6	0.40
25%	0.6	560.4	1745.4	1075.7	0.93
50%	0.9	617.3	2037.3	1358.5	1.16
75%	1.4	733.1	2289.7	1631.5	1.46
Max	2.0	973.2	3809.3	3792.3	2.82

Seven predictive variables were used in the model: the prescription dose, DIBH amplitude, heart volume, lung volume, the volume of tissue receiving > =90% of the prescription dose (V90%), planned MHD and the shift in heart position. Each variable was chosen as it was deemed likely to be predictive of the shifted MHD. For this study, the DIBH amplitude was calculated using each patient's breathing trace recorded using the Varian (Palo Alto, CA) Real-Time Position Management (RPM) system. Threshold bars are set +/–2.5 mm around the patient's stable breath-hold amplitude and the DIBH amplitude calculated as the distance between the patient's free-breathing baseline and the lowest threshold bar amplitude.

Of the seven parameters, the dose prescription for each patient was either 40 Gy/15# or 50 Gy/25# and the shifts taken were either 3 mm, 5 mm and 7 mm. The remaining five parameters were continuous in nature and are best described by the summary statistics outlined in Table 1 below.

2.2. Neural network

The neural network was trained and optimised on data from 50 patients using Keras (https://keras.io/). Keras is developed with a focus on enabling fast experimentation and allows a simple approach to the design and training of neural networks. It is written in Python and runs on top of TensorFlow, Google's open-source software for deep learning [37,38]. A neural network is typically composed of computational layers that process data in a hierarchical fashion. Each layer takes an input and produces an output, often computed as a non-linear function of a weighted linear combination of the input values as shown in Fig. 2. The output of one layer becomes an input to the next processing layer [37–39]. To find the optimal the parameters for our network, Keras uses back-projection to find parameters w_1 to w_n, and b_1 to b_n that minimize the error on our training data.

2.3. Cross-validation

Network evaluation followed a k-fold cross-validation schema. As the first step, data from 50 patients were randomly separated into a random train/test split of 90%/10%. For each split, 90% of the data was used for predictor training, while the remaining 10% was used for testing model performance. To ensure we were not "lucky" in our initial split used for training and testing, we repeated the validation procedure for 20 random training–testing separations. For each train/test split, all previously trained information was completely erased from the model so that each trained model was unfamiliar with the previously trained data. This process was used to test different network architectures to find the most optimal network architecture and to evaluate the performance of our final network. However, using the results from cross-validation to make decisions regarding network architecture may inadvertently bias the network towards the test data. To ensure the decisions made by the authors were not directly influenced by the results

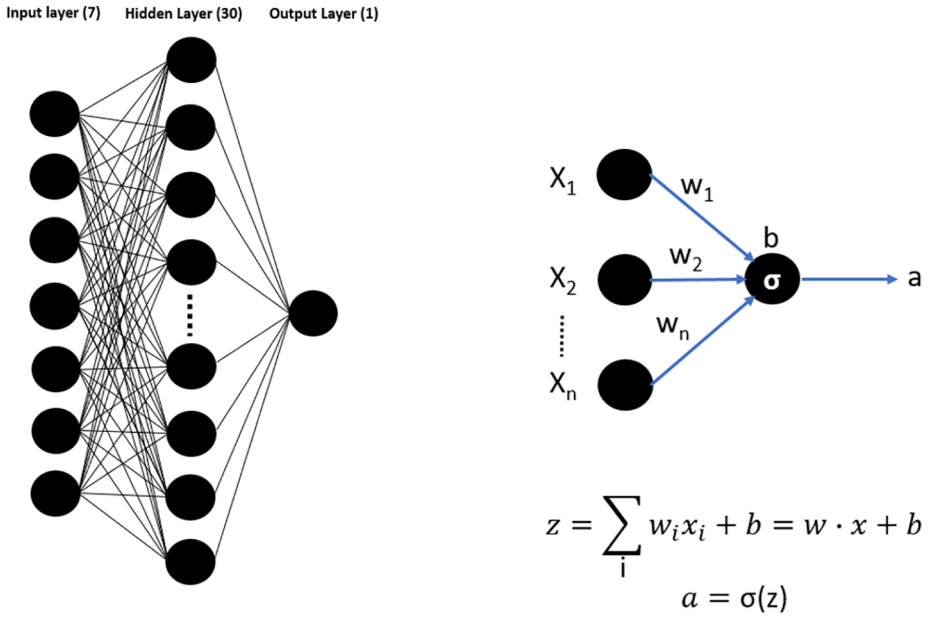

Fig. 2. x_i = Input value, w_i = Input weight, b = Bias term (threshold), σ = Activation function, a = Output value.

of the test data during the network optimisation phase, an additional 15 patients were included in the study to independently verify the final network performance.

2.4. Network optimisation

To determine the optimal network, both the number of layers (i.e. depth) and neurons (i.e. width) were varied. The number of neurons was increased incrementally from 1 to 60 and the number of hidden layers increased from 1 to 3. Sigmoid, linear and Relu activation functions also were evaluated to find the most optimal activation function for the hidden layers. Cross-validation was undertaken to evaluate each network architecture on unseen data not used in training the network. The root mean squared prediction error (RMSE) and the maximum error in prediction from twenty models trained and tested using cross-validation was used to represent the performance of each network architecture to new data [40]. The neural network architecture which obtained the lowest RMSE and lowest maximum error during the cross-validation stage was deemed to be the optimal network for predicting the MHD.

2.5. Model training and assessment

Once the most optimal network architecture was found, we progressed to the training and validation phase and set up a fully connected 3-layer neural network as shown in Fig. 2. The first layer contains 7 neurons representing the 7 input parameters of the model. The second "hidden" layer contains 30 neurons, found to be optimal from our network optimisation phase. As we want a single estimate based on our input parameters, the last layer is represented by a single neuron. The "Relu" activation function was utilised for the hidden layer only and all weights and biases were initialised as "uniform". The training was undertaken over 5000 epochs using the "mean squared error" loss function and "Adam" optimizer. To prevent overfitting, early stopping was enabled to stop the network training when the validation loss was stable over 10 epochs [40]. A Gaussian noise regularization layer was also utilized, as added noise has been shown to achieve lower training loss by encouraging active exploration of parameter space [41]. The Keras documentation also describes the Gaussian noise layer as a method to prevent overfitting. The RMSE and maximum prediction error of our optimal network were found with cross-validation to test whether the final optimised network performs well on new data not previously used for training. Lastly, to verify the results from our cross-validation on 50 patients, the network was used to predict the shifted MHD for 15 additional completely independent patients not previously used for either optimising network architecture or training the network.

3. Results

3.1. Data exploration

The average planned MHD was 1.3 Gy +/–0.5 Gy (1SD). A shift of 3 mm, 5 mm and 7 mm resulted in an average shifted MHD of 1.8 Gy +/–0.8 Gy (1SD), 2.1 Gy +/–0.9 Gy (1SD) and 2.5 Gy +/–1.0 Gy (1SD) respectively. Our initial assessment of the raw data shows the MHD increased in a linear fashion and that the rate of change tended to increase with the initial MHD (Fig. 3). Only the initial planned MHD had a strong linear correlation ($r > 0.9$) with the shifted MHD. The lung volume, V90% and prescription dose had weak correlations ($r > 0.3$) while the DIBH amplitude and heart volume showed no linear

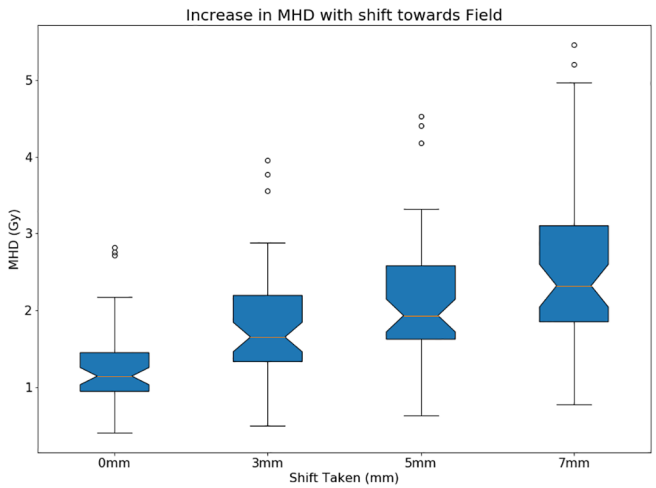

Fig. 3. Results from each shifted heart are shown. The approximately linear increase in MHD can be seen for each patient when the heart is shifted 0 mm (planned position), 3 mm, 5 mm and 7 mm from its original planned position.

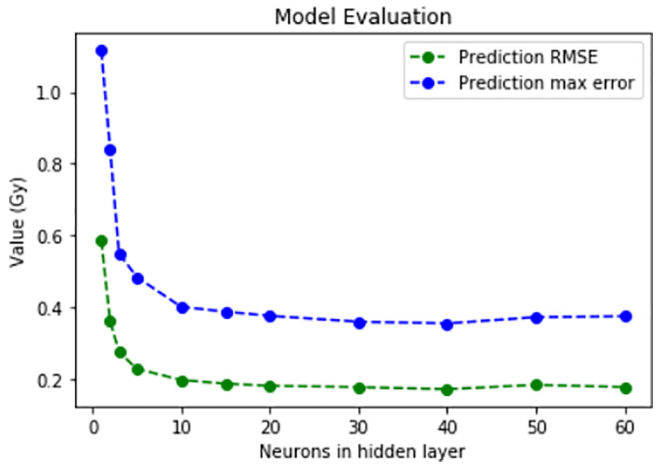

Fig. 4. Variation of network prediction ability with the number of hidden layer neurons.

correlation. Utilising these parameters in a neural network enables us to evaluate both linear and non-linear relationships between parameters, ensuring that any relationship between parameters that aid the prediction of the shifted MHD would be weighted higher than those that have little or no predictive relationship.

3.2. Model assessment

Increasing the number of hidden layers between 1 and 3 demonstrated that one single hidden layer was optimal for our data. No additional benefit was found when multiple additional hidden layers were used. However, the prediction ability of the network changed depending on the number of neurons in the hidden layer. The model prediction ability increased significantly when the number of neurons increased from 1 to 10, a very slight improvement was noted from 10 to 30 neurons and no extra improvement was found above 30 neurons, as shown in Fig. 4. Good cross-validation results were found using an early stopping patience variable of 10 epochs, increasing the number further didn't yield better prediction results and increases the likelihood of overfitting. The ReLU activation function consistently resulted in a lower RMSE and maximum prediction error compared to both linear and sigmoid activation functions and was used for the final model.

3.3. Model prediction accuracy

Results from 20 random train/test splits from our optimal network are shown in Fig. 5. Of a total 150 data points, 15 (10%) were used for testing on each train/test split resulting in a total of 300 predictions. Using the model described, 94% of all prediction errors were below 0.2 Gy, 97.3% were below 0.3 Gy and 100% were below 0.5 Gy. The average RMSE and maximum prediction error over all train/test splits were 0.13 Gy and 0.5 Gy respectively. Additional data from 15 completely independent patients resulted in predictions that correlated well with our cross-validation results. For shifts of 3 mm, 5 mm and 7 mm, 92.2% of all prediction errors were below 0.2 Gy, 97.4% were below 0.3 Gy and 100% were below 0.5 Gy. This confirms that the model performed as expected on new data and our decisions regarding network architecture did not favour test data.

4. Discussion

For left-sided breast cancer patients, mean heart dose is related to the distance between the heart and the treatment field. When this relationship changes during treatment, the increase in dose to the heart can be difficult to estimate. Traditionally, to evaluate the dosimetric impact of a difference in heart position, the imaging would first be repeated to evaluate consistency. If the heart position is consistent, a Cone Beam CT (CBCT) would be undertaken and the dosimetric impact evaluated by a Physicist. This process typically takes a number of days to complete and as patients typically receive treatment over 15–25 fractions, the patient would have received a large portion of their treatment before action is taken, reducing the impact of any intervention taken to rectify the issue. Alternatively, using the maximum heart distance to predict the mean heart dose has been shown to be prone to large uncertainties [27,28,36].

We have demonstrated that a neural network is a valid method to predict the increase in MHD when a deviation in heart position is noted during treatment. Prediction accuracy was found to be good as 94% of all prediction errors were below 0.2 Gy, 97.3% were below 0.3 Gy and 100% were below 0.5 Gy. The average RMSE and maximum prediction error over all train/test splits were 0.13 Gy and 0.5 Gy respectively. Based on the relationship between dose and risk of ischemic heart disease found by Darby et al [33], a prediction error of 0.2 Gy, 0.3 Gy and 0.5 Gy corresponds to a 1.5%, 2.2% and 3.7% increased risk of ischemic heart disease.

The uncertainty in measuring the shifted MHD was considered and found to be +/–0.12 Gy which would result in the network including

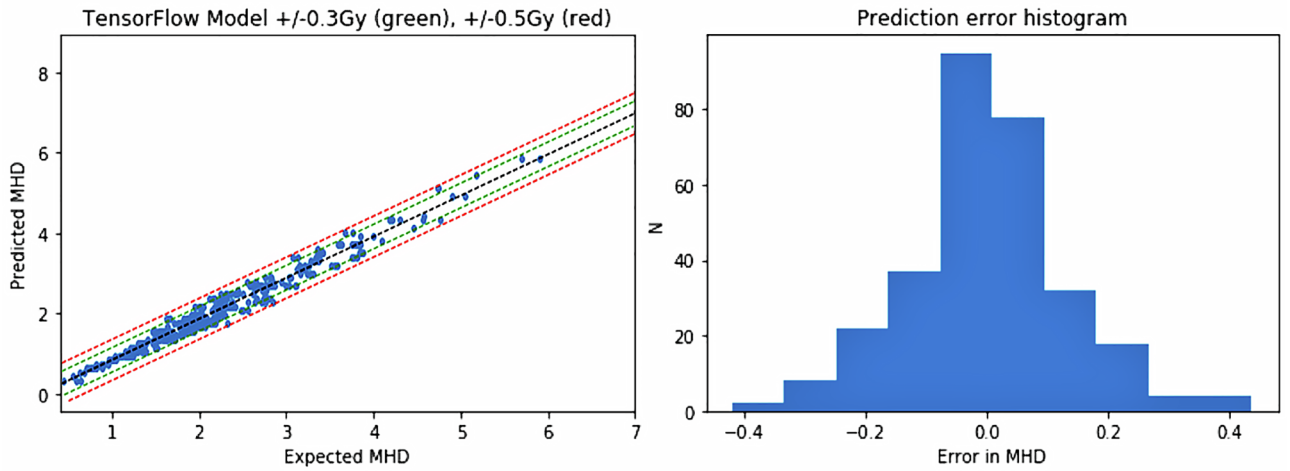

Fig. 5. Left: Prediction vs. Expected values. Error bars represent a prediction error level of +/–0.3% (green) and +/–0.5 Gy (red). Right: Histogram of all prediction errors in Gray.

this “noise” during training. To reduce this noise, an increased sample of patients could be used to further refine the prediction ability of the trained network.

These results are a significant improvement on previous studies using traditional prediction methods. Taylor et al and Kong et al found the maximum heart distance (d), defined as the maximum measure of heart protruding into the medial field, could be used as a predictor of the mean heart dose. Taylor et al’s results showed a prediction ability within 0.7 Gy_2 for 90% of patients and within 1.4 Gy_2 for 100% of patients. E.L. Lorenzen et al further investigated this relationship using linear regression analysis and found the relationship to be 2.43 Gy/cm (d) + 0.42 Gy with a RMSE ranging from 0.5 Gy to 4.5 Gy depending on the approach used.

The neural network used in this study was comprised of a single hidden layer with commonly used regularisation methods and parameters. Using Keras enabled fast experimentation for both optimizing the network architecture and validating the network. Keras also enables the user to query the weightings found during training such that the most predictive parameters, from the perspective of the neural network, can be obtained. We found that the planned MHD was the strongest parameter, which makes sense considering the relationship between how quickly the MHD increases with distance and the initial planned MHD in Fig. 3. The V90% was also strongly predictive, followed by the prescription dose, lung volume and lastly the heart volume. Each neuron in the hidden layer possessed a different combination of input parameter weightings corresponding to the different predictive relationships between the input variables. Investigating the weightings found by Keras for our single hidden layer neural network allows for interpretation of what inputs the network found to be most predictive. However, networks of higher complexity would be difficult to interpret in this manner.

Our approach using a neural network provides a clinically acceptable estimate of the increase in MHD, without the need for further imaging, contouring or evaluation. A clinician can provide an action level tolerance for treatment staff to follow when preforming pre-treatment imaging. Estimated heart deviations below this tolerance allow the treatment staff to monitor the heart position with confidence that a serious dose deviation is not occurring.

5. Conclusions

We described a novel method to predict the change in MHD using a neural network when a deviation in heart position is noted during the treatment of left-sided DIBH breast cancer cases. The prediction is based on a number of parameters readily available at time of treatment planning. An optimal neural network was found by varying model parameters and using cross-validation to evaluate each models’ prediction ability. The trained neural network gives clinicians the information and tools required to evaluate what shift in heart position would be acceptable and which scenarios require immediate action before treatment commences. Also, the resources and time typically associated with following up these issues would be greatly reduced as no additional contouring or calculations are required, only parameters in the patient’s treatment plan. Cross-validation shows the neural network is generalisable to new data with a RMSE of 0.13 Gy and maximum error in prediction < 0.5 Gy. Results were related back to clinical risk models presented in the literature. Finally, we have shown that neural networks offer improved prediction abilities compared to traditional approaches for predicting the MHD for DIBH breast cancer cases.

References

[1] Feng M, Valdes G, Dixit N, Solberg TD. Machine Learning in Radiation Oncology: Opportunities, Requirements, and Needs. Front Oncol 2018;8:1–7. https://doi.org/10.3389/fonc.2018.00110.

[2] Kang J, Schwartz R, Flickinger J, Beriwal S. Machine learning approaches for predicting radiation therapy outcomes: a clinician’s perspective. Int J Radiat Oncol Biol Phys 2015;93:1127–35. https://doi.org/10.1016/j.ijrobp.2015.07.2286.

[3] Kortesniemi M, Tsapaki V, Trianni A, Russo P, Maas A, Källman HE, et al. The European Federation of Organisations for Medical Physics (EFOMP) White Paper: big data and deep learning in medical imaging and in relation to medical physics profession. Phys Medica 2018;56:90–3. https://doi.org/10.1016/j.ejmp.2018.11.005.

[4] Varfalvy N, Piron O, Cyr MF, Dagnault AAL. Classification of changes occurring in lung patient during radiotherapy using relative γ analysis and hidden Markov models. Int J Lab Hematol 2016;38:42–9. https://doi.org/10.1111/ijlh.12426.

[5] Oakden-Rayner L, Carneiro G, Bessen T, Nascimento JC, Bradley AP, Palmer LJ. Precision Radiology: predicting longevity using feature engineering and deep learning methods in a radiomics framework. Sci Rep 2017;7:1–13. https://doi.org/10.1038/s41598-017-01931-w.

[6] Lao J, Chen Y, Li ZC, Li Q, Zhang J, Liu J, et al. A Deep Learning-Based Radiomics Model for Prediction of Survival in Glioblastoma Multiforme. Sci Rep 2017;7:1–8. https://doi.org/10.1038/s41598-017-10649-8.

[7] Li Z, Wang Y, Yu J, Guo Y, Cao W. Deep Learning based Radiomics (DLR) and its usage in noninvasive IDH1 prediction for low grade glioma. Sci Rep 2017;7:1–11. https://doi.org/10.1038/s41598-017-05848-2.

[8] Cha KH, Hadjiiski L, Chan HP, Weizer AZ, Alva A, Cohan RH, et al. Bladder Cancer Treatment Response Assessment in CT using Radiomics with Deep-Learning. Sci Rep 2017;7:1–12. https://doi.org/10.1038/s41598-017-09315-w.

[9] Tseng HH, Luo Y, Cui S, Chien JT, Ten Haken RK, NI. Deep Reinforcement Learning for Automated Radiation Adaptation in Lung Cancer Huan-Hsin. Int J Lab Hematol 2016;38:42–9. https://doi.org/10.1111/ijlh.12426.

[10] Sharp G, Fritscher KD, Pekar V, Peroni M, Shusharina N, Veeraraghavan H, et al. Vision 20/20: perspectives on automated image segmentation for radiotherapy. Med Phys 2014;41:1–13. https://doi.org/10.1118/1.4871620.

[11] Dai W, Dong N, Wang Z, Liang X, Zhang H, Xing EP. 2018. Scan: Structure correcting adversarial network for organ segmentation in chest x-rays. Lect Notes Comput Sci (Including Subser Lect Notes Artif Intell Lect Notes Bioinformatics) 11045 LNCS:263–73. doi:10.1007/978-3-030-00889-5_30.

[12] Ibragimov B, Xing L. Segmentation of organs-at-risks in head and neck CT images using convolutional neural networks. Med Phys 2017;44:547–57. https://doi.org/10.1002/mp.12045.

[13] Korfiatis P, Kline TL, Lachance DH, Parney IF, Buckner JC, Erickson BJ. Residual Deep Convolutional Neural Network Predicts MGMT Methylation Status. J Digit Imaging 2017;30:622–8. https://doi.org/10.1007/s10278-017-0009-z.

[14] Ruan D, Keall P. Online prediction of respiratory motion: Multidimensional processing with low-dimensional feature learning. Phys Med Biol 2010;55:3011–25. https://doi.org/10.1088/0031-9155/55/11/002.

[15] Isaksson M, Jalden J, Murphy MJ. On using an adaptive neural network to predict lung tumor motion during respiration for radiotherapy applications. Med Phys 2005;32:3801–9. https://doi.org/10.1118/1.2134958.

[16] Mori S. Deep architecture neural network-based real-time image processing for image-guided radiotherapy. Phys Medica 2017;40:79–87. https://doi.org/10.1016/j.ejmp.2017.07.013.

[17] Li Q, Chan MF. Predictive time-series modeling using artificial neural networks for Linac beam symmetry: an empirical study. Ann N Y Acad Sci 2017;1387:84–94. https://doi.org/10.1111/nyas.13215.

[18] Valdes G, Scheuermann R, Hung CY, Olszanski A, Bellerive M, Solberg TD. A mathematical framework for virtual IMRT QA using machine learning. Med Phys 2016;43:4323–34. https://doi.org/10.1118/1.4953835.

[19] Valdes G, Chan MF, Lim SB, Scheuermann R, Deasy JO, Solberg TD. IMRT QA using machine learning: a multi-institutional validation. J Appl Clin Med Phys 2017;18:279–84. https://doi.org/10.1002/acm2.12161.

[20] El Naqa I, Ruan D, Valdes G, Dekker A, McNutt T, Ge Y, et al. Machine learning and modeling: data, validation, communication challenges. Med Phys 2018. https://doi.org/10.1002/mp.12811.

[21] Ferlay J, Soerjomataram I, Ervik M, Dikshit R, Cancer Eser S MC, et al. Incidence and Mortality Worldwide: IARC CancerBase No. 11e. GLOBOCAN; 2012.

[22] Darby S, McGale P, Correa C, Taylor C, Arriagada R, Clarke M, et al. Effect of radiotherapy after breast-conserving surgery on 10-year recurrence and 15-year breast cancer death: meta-analysis of individual patient data for 10 801 women in 17 randomised trials. Lancet 2011;378:1707–16. https://doi.org/10.1016/S0140-6736(11)61629-2.

[23] Abe O, Abe R, Enomoto K, Kikuchi K, Koyama H, Masuda H, et al. Effects of radiotherapy and of differences in the extent of surgery for early breast cancer on local recurrence and 15-year survival: an overview of the randomised trials. Lancet 2005;366:2087–106. https://doi.org/10.1016/S0140-6736(05)67887-7.

[24] Ozyigit G. Current role of modern radiotherapy techniques in the management of breast cancer. World J Clin Oncol 2014;5:425. https://doi.org/10.5306/wjco.v5.i3.425.
[25] Syriopoulou E, Bower H, Andersson TML, Lambert PC, Rutherford MJ. Estimating the impact of a cancer diagnosis on life expectancy by socio-economic group for a range of cancer types in England. Br J Cancer 2017;117:1419–26. https://doi.org/10.1038/bjc.2017.300.
[26] Hooning MJ, Aleman BMP, Van Rosmalen AJM, Kuenen MA, Klijn JGM, Van Leeuwen FE. Cause-specific mortality in long-term survivors of breast cancer: a 25-year follow-up study. Int J Radiat Oncol Biol Phys 2006;64:1081–91. https://doi.org/10.1016/j.ijrobp.2005.10.022.
[27] Taylor CW, McGale P, Povall JM, Thomas E, Kumar S, Dodwell D, et al. Estimating Cardiac Exposure From Breast Cancer Radiotherapy in Clinical Practice. Int J Radiat Oncol Biol Phys 2009;73:1061–8. https://doi.org/10.1016/j.ijrobp.2008.05.066.
[28] Lorenzen EL, Brink C, Taylor CW, Darby SC, Ewertz M. Uncertainties in estimating heart doses from 2D-tangential breast cancer radiotherapy. Radiother Oncol 2016;119:71–6. https://doi.org/10.1016/j.radonc.2016.02.017.
[29] Gagliardi Giovanna, Constine Louis S, Moiseenko Vitali, Correa Candace, Pierce Lori J, Allen Aaron M, et al. Radiation Dose–Volume Effects In The Heart. Int J Radiat Oncol Biol Phys 2010;76:77–85. https://doi.org/10.1016/j.ijrobp.2009.05.070.
[30] Rudra Sonali, Al-Hallaq Hania A, Feng Christine, Chmura Steven J, Y, Hasan. Effect of RTOG breast/chest wall guidelines on dose-volume histogram parameters. J Appl Clin Med Phys 2014;15:4547. https://doi.org/10.1111/j.1743-6109.2008.01122.x. Endothelial.
[31] Bergom C, Currey A, Desai N, Tai A, Strauss JB. Deep Inspiration Breath Hold: Techniques and Advantages for Cardiac Sparing During Breast Cancer Irradiation. Front Oncol 2018;8:1–10. https://doi.org/10.3389/fonc.2018.00087.
[32] Royal College of Radiologists. Postoperative radiotherapy for breast cancer. UK consensus statements 2016.
[33] Darby SC, Ewertz M, McGale P, Bennet AM, Blom-Goldman U, Brønnum D, et al. Risk of Ischemic Heart Disease in Women after Radiotherapy for Breast Cancer. N Engl J Med 2013;368:987–98. https://doi.org/10.1056/NEJMoa1209825.
[34] Huppert N, Jozsef G, DeWyngaert K, Formenti SC. The Role of a Prone Setup in Breast Radiation Therapy. Front Oncol 2011;1:1–8. https://doi.org/10.3389/fonc.2011.00031.
[35] Joseph K, Warkentin H, Ghosh S, Polkosnik LA, Powell K, Brennan M, et al. Cardiac-sparing radiation therapy using positioning breast shell for patients with left-sided breast cancer who are ineligible for breath-hold techniques. Adv Radiat Oncol 2017;2:532–9. https://doi.org/10.1016/j.adro.2017.08.002.
[36] Kong FM, Klein EE, Bradley JD, Mansur DB, Taylor ME, Perez CA, et al. The impact of central lung distance, maximal heart distance, and radiation technique on the volumetric dose of the lung and heart for intact breast radiation. Int J Radiat Oncol Biol Phys 2002;54:963–71. https://doi.org/10.1016/S0360-3016(02)03741-0.
[37] Abadi M, Agarwal A, Barham P, Brevdo E, Chen Z, Citro C, et al. TensorFlow: Large-Scale Machine Learning on Heterogeneous. Distributed Systems 2016. https://doi.org/10.1038/nn.3331.
[38] Abadi Martín, Barham Paul, Chen Jianmin, Chen Zhifeng, Davis Andy, Dean Jeffrey, et al. and Xiaoqiang Zheng GB. TensorFlow: A System for Large-Scale Machine Learning. Nat Neurosci 2013;16:486–92. https://doi.org/10.1038/nn.3331.
[39] Rampasek L, Goldenberg A. TensorFlow: Biology's Gateway to Deep Learning? CellSyst 2016;2:12–4. https://doi.org/10.1016/j.cels.2016.01.009.
[40] Caruana R, Lawrence S, Giles L. Overfitting in neural nets: Backpropagation, conjugate gradient, and early stopping. 13th Int Conf Neural Inf Process Syst 2000:402–8. https://doi.org/10.1109/IJCNN.2000.857823.
[41] Neelakantan A, Vilnis L, Le QV, Sutskever I, Kaiser L, Kurach K, et al. Adding Gradient Noise Improves Learning for Very Deep. Networks 2015:1–11. https://doi.org/10.21437/Interspeech.2016-491.